Electrochemical Behavior of Poly(ferrocenyldimethylsilane-*b*-dimethylsiloxane) Films

Tao Chen, Li Wang,* Guohua Jiang, Jianjun Wang, Xiaochen Dong, Xuejie Wang, Junfeng Zhou, Chiliang Wang, and Wei Wang

State Key Lab of Polymer Reaction Engineering, Zhejiang University, Hangzhou 310027, People's Republic of China

Received: August 27, 2004; In Final Form: January 9, 2005

The electrochemical behavior of poly(ferrocenyldimethylsilane-*b*-dimethylsiloxane) (PFDMS-*b*-PDMS) films deposited on a glassy carbon electrode was investigated by means of cyclic voltammetry (CV). The influences of the solvent, film thickness, temperature, and PDMS block length in PFDMS-*b*-PDMS on the electrode process were discussed. It was found that in 0.1 M aqueous $LiClO_4$ the electrochemical processes of the films on a glassy carbon electrode were complex and have a low rate of electron transport and mass diffusion. The kinetic parameters obtained indicated that the electrode process was controlled by both the electrode reaction and mass diffusion.

Introduction

Polymers containing organoferrocenyl units in the main chain are of considerable interest since they possess unique characteristics and potential appliance foreground because of their unique redox, electrical, magnetic, and other characteristics.[1−15] For example, it was found that all synthesized polyferrocenylsilanes exhibit unique electrochemical activity.[9,10] In our previous papers,[10,16,17] we reported that various supporting electrolytes have a remarkable influence on the electrochemical behavior and stabilization of the polyferrocenylsilane films. Electrochemical studies of organoferrocenyl block polymers will help us understand the relationship between the structure and property of the block copolymer. These studies are important in developing novel polymer materials and their applications for modified electrodes and electrochemical sensors. However, to our knowledge, few detailed electrochemical studies have been reported for polyferrocene block copolymers.[18−21] In this paper, we report on the electrochemical behavior of a poly(ferrocenyldimethylsilane-*b*-dimethylsiloxane) (PFDMS-*b*-PDMS) block copolymer film deposited onto a glassy carbon electrode in aqueous $LiClO_4$.

Experimental Section

Instruments and Reagents. The cyclic voltammetry (CV) measurements were carried out with a CHI-630A Electrochemical Analyzer (CH Instruments, Inc., Austin, TX) in an undivided three-electrode cell. All electrodes were from CH Instruments. A platinum wire counter electrode and a Ag−AgCl (3 M KCl) reference electrode were used. The working electrode was a Teflon-shrouded glassy carbon disk electrode (ϕ = 3 mm, geometric area = 0.071 cm^2) which was polished to a mirror finish with 0.05-μm Al_2O_3 paste on felt and cleaned by ultrasonication successively in 0.1 M NaOH, 1:1 HNO_3/anhydrous ethyl alcohol, and double-distilled water. Then it was dried and used for electrochemical measurements. The solutions were filtered with a 0.45-μm micropore filter and purged for 15 min with prepurified nitrogen before use.[16,17]

Synthesis and Characterization. PFDMS-*b*-PDMS was synthesized according to the literature,[13] and ^{1}HNMR spectra of polymers were recorded with a 500 MHz AVANCE NMR spectrometer (model DMX500) in $CDCl_3$ using TMS as the standard.

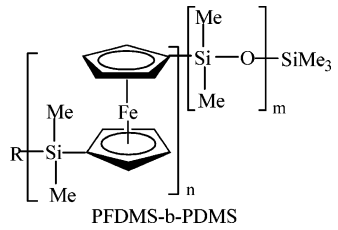

PFDMS-b-PDMS

Figure 1. Structure of PFDMS-*b*-PDMS.

TABLE 1: Molecular Characteristics of PFDMS-*b*-PDMS

block copolymer	PFDMS content (mol %)[b]	M_n (g mol^{-1})[c]	M_w/M_n[c]
$PFDMS_{20}$-*b*-$PDMS_{200}$[a]	9.1	1.9×10^4	1.06
$PFDMS_8$-*b*-$PDMS_{270}$[a]	2.9	2.2×10^4	1.50

[a] The number shows the average number of polymerization degrees foreach block. [b] The PFDMS content was determined by NMR and GPC. [c] M_n was determined by GPC.

The molecular weight was determined by gel permeation chromatography (GPC) with a laser scattering detector and an Ultrastyragel column with pore sizes of 10^3-10^5 Å. The eluent was THF at a flow rate of 1.0 mL min^{-1}. A detection wavelength of 632.8 nm and the refraction index increment value of the polymer solutions d*n*/d*c* = 0.20 were used for laser scattering detection.

PFDMS-*b*-PDMS Film-Coated Electrodes. PFDMS-*b*-PDMS-coated electrodes were prepared by covering the glassy carbon disk electrodes with a solution of PFDMS-*b*-PDMS in THF, and then the solvent was evaporated at 25 °C.

Results and Discussion

Characterization of PFDMS-*b*-PDMS. The structure of PFDMS-*b*-PDMS is shown in Figure 1, and the molecular weight of PFDMS-*b*-PDMS is shown in Table 1. The ^{1}H NMR (500 MHz, in $CDCl_3$) spectrum of PFDMS-*b*-PDMS showed peaks with the following shifts: 0.39 (H, in $-CH_3$ [(η-$C_5H_4)_2$-$FeSiMe_2$]), 4.35 and 4.10 (in $-C_5H_4$), and 0.07 (H, in $-CH_3$ [Me_2SiO]).

* Corresponding author. E-mail: opl_wl@dial.zju.edu.cn. Fax: +86-571-87951612.

10.1021/jp0461246 CCC: $30.25
Published on Web 02/15/2005

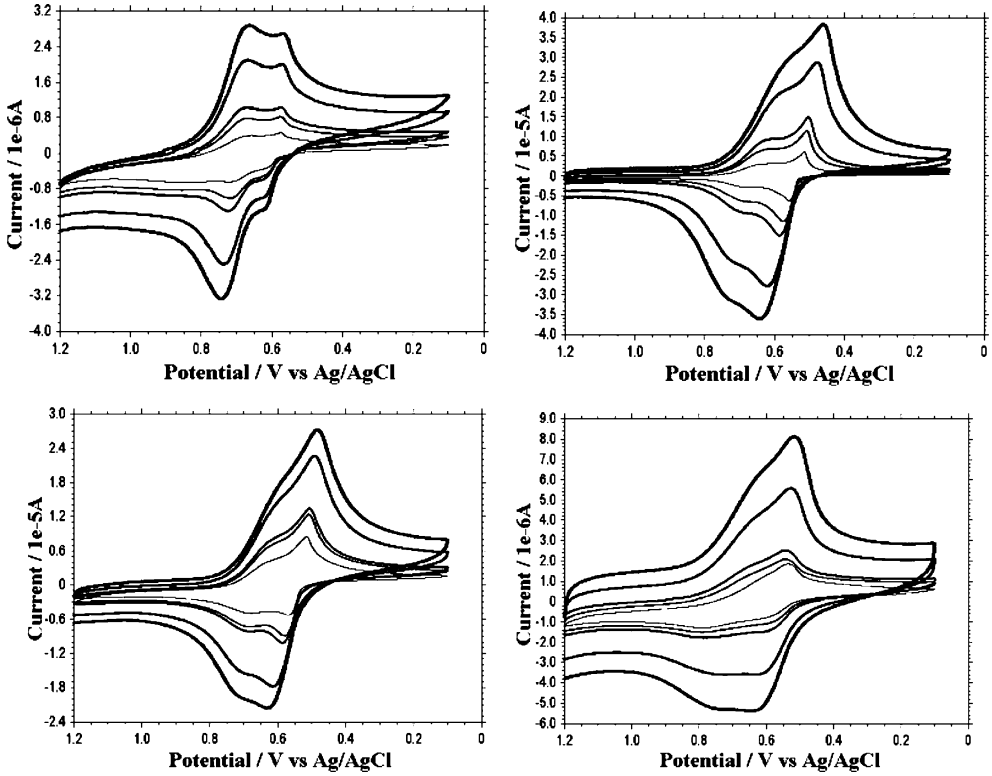

Figure 2. Cyclic voltammograms of a $PFDMS_{20}$-*b*-$PDMS_{200}$ film in different solvents. Coverage Γ is ca. 6.5×10^{-7} mol cm^{-2} of the ferrocene site in 0.1 M $LiClO_4$ at a scan rate of 20, 40, 60, 80, and 100 mV s^{-1} from inner to outer at 25 °C: (a) H_2O, (b) C_2H_5OH, (c) *i*-C_3H_7OH, and (d) *n*-C_4H_9OH.

TABLE 2: Dielectric Constant and Viscosity of Solvents

parameter	water	ethanol	2-propanol	*n*-butanol	acetonitrile	ethyl acetate
dielectric constant (25 °C)	78.54	24.3	18.3	17.1	37.5 (20 °C)	6.02
viscosity (20 °C, mPa S^{-1})	0.8937	1.17	2.1	3.379 (15 °C)	0.340 (25 °C)	0.441 (25 °C)

TABLE 3: Electrochemical Data of the $PFDMS_{20}$-*b*-$PDMS_{200}$ Film in Some Solvents[a]

solvent	$E_{1/2}(1)$	$E_{1/2}(2)$	ΔE
water	0.626	0.724	0.098
ethanol	0.642	0.743	0.101
2-propanol	0.627	0.731	0.104
n-butanol	0.614	0.764	0.150
acetonitrile	0.818	1.061	0.243
ethyl acetate	0.697	0.937	0.240

[a] Coverage Γ is ca. 6.5×10^{-7} mol cm^{-2} of the ferrocene site in 0.1 M $LiClO_4$ at a scan rate of 100 mV s^{-1}.

Effect of Solvent on CV Behavior of the PFDMS-*b*-PDMS Film. PFDMS-*b*-PDMS has the special dissolving property; namely, it cannot be dissolved in water, low-grade alcohol, and acetonitrile with strong polarity, but it can be dissolved in ether with lower polarity, chloroalkanes, and benzene. Thus, it exhibits different CV behaviors in different solvents.

Water, ethanol, 2-propanol, *n*-butanol, acetonitrile, and ethyl acetate were used as solvents to study the electrochemical behavior of films. Their physical parameters are listed in Table 2. The CV behavior and electrochemical data from $PFDMS_{20}$-*b*-$PDMS_{200}$ film in different solvents are shown in Figure 2 and Table 3, respectively.

Figure 2 shows that the solvent has a remarkable effect on the electrochemical behavior of the $PFDMS_{20}$-*b*-$PDMS_{200}$ film. In water, ethanol, 2-propanol, and *n*-butanol, the CV peak currents of the $PFDMS_{20}$-*b*-$PDMS_{200}$ film increased gradually with the initial and each successive sweep, until it reached a steady state at which stable and reproducible current−potential curves were obtained. The CV behavior of the $PFDMS_{20}$-*b*-$PDMS_{200}$ film in water exhibited a double peak, and in other solvents, the double peak gradually became a single peak, which indicates that the $PFDMS_{20}$-*b*-$PDMS_{200}$ film exhibits different electrochemical behaviors on a glassy carbon electrode in different solvents. Moreover, as can be seen from Table 3, the peak separation of ΔE increased gradually as the dielectric constant falls. The peak separation is indicative of the degree of interaction between the metal centers. In ethanol, 2-propanol, and *n*-butanol, the swollen behavior of PFDMS-*b*-PDMS film decreased gradually; as a result ion penetration into the film becomes difficult. Also, the CV signal was found to attenuate gradually in acetonitrile and ethyl acetate, which indicates that, for those solvents, the $PFDMS_{20}$-*b*-$PDMS_{200}$ film has a very high swollen behavior and dissolved in those solvents.

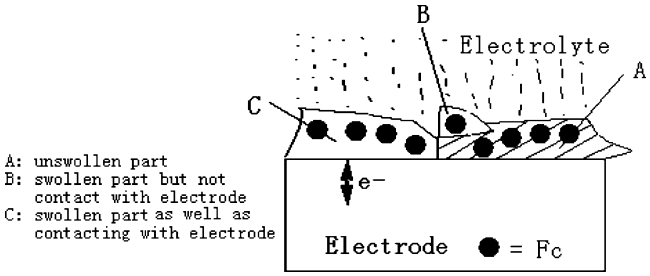

Figure 3. Sketch map of charge transfer and polymer on the glassy carbon disk electrode.

The above results indicate that the solvent-swollen polymer films and the penetration of solvated electrolyte ions play an important role in film electrode processes (Figure 3). In Figure 3, A shows the unswollen parts of the film where the electrolyte

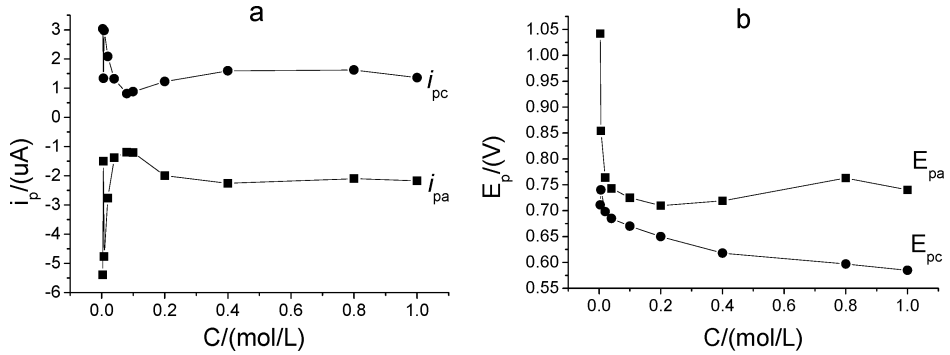

Figure 4. Influences of $LiClO_4$ aqueous concentration on i_p and E_p of the $PFDMS_{20}$-*b*-$PDMS_{200}$ film. Coverage Γ is ca. 6.5×10^{-7} mol cm^{-2} of the ferrocene site at a scan rate of 100 mV s^{-1} at 25 °C.

cannot swell it and the redox site in the unswollen region is not electrochemically active. Although B is swollen, it also cannot transfer electrons from the electrode surface to electrolyte because it does not make contact with the electrode; only C can transfer electrons because it possesses the swollen parts and contacts the electrode. As a consequence of the incorporation of ions and solvent molecules into the film, swelling of the polymer matrix can take place. The originally neutral polymer film is transformed into a swollen polyelectrolyte gel. Along with the increasing electrolyte concentration, the ohmic resistance of the solution decreases and the ion concentration and the diffusion rate of the electroactive species increase in the film. The different solvents made the PFDMS-*b*-PDMS films possess different soluble statuses. Thus, solvent has important influence on the electrochemical behavior of a PFDMS-*b*-PDMS film.

Effect of Electrolyte Concentration on the CV Behavior of the PFDMS-*b*-PDMS Film. The influence of $LiClO_4$ concentration in the supporting electrolyte on the CV process was investigated, and the results are shown in Figure 4. When concentrations were greater than 0.08 M, the electrolyte concentration had no more influence on peak currents and peak potentials. But at very low concentrations, the peak current, i_p, increased with increasing electrolyte concentration. When the concentration was about 0.008 M, the peak currents reached the maximum, then decayed, and gradually became stable. Similarly, in the low-concentration region, with increasing concentration, the oxidation peak moved toward lower potentials, while the reduction peak moved toward higher potentials; thus, the peak-to-peak separation, ΔE_P, increased and then gradually stabilized. Moreover, oxidation peak current i_{pa} and oxidation peak potential E_{pa} changed with electrolyte concentration much more than those corresponding to reduction peaks; hence, the influence of electrolyte concentration on the oxidation process was more significant. The reason is the oxidation process in these polymer films is limited by ionic transport rate. The oxidation product, poly(ferricenium), is ionic, and the kinetics of oxidation in these films is limited by counterion flow into and out of the polymer phase.

Effect of Film Thickness on CV Behavior of the PFDMS-*b*-PDMS Film. Film thickness also had a major effect on the cyclic voltammograms. At different film thicknesses, there were significant differences in peak shapes, peak currents, and peak potentials. The PFDMS-*b*-PDMS film in 0.1 M aqueous $LiClO_4$ exhibited two pairs of oxidation−reduction peaks and possessed good CV peak shapes, similar to CV waves of poly(ferrocenylsilane) solutions,[22−25] only at moderate apparent coverage. However, at low and high coverage, the oxidation peaks were sharper than the reduction peaks, and oxidation peak current i_{pa} was larger than reduction peak current i_{pc}. Typical cyclic

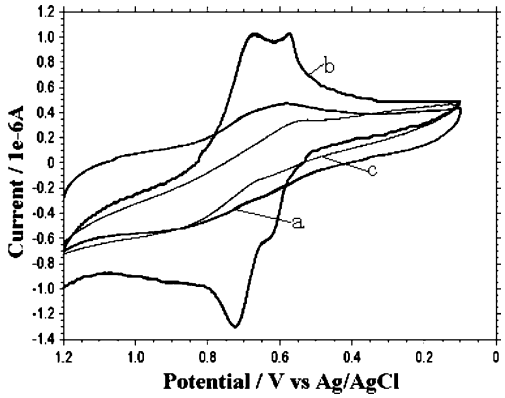

Figure 5. Cyclic voltammograms of the $FDMS_{20}$-*b*-$PDMS_{200}$ film in aqueous 0.1 M $LiClO_4$, potential scan rate $\upsilon = 0.1$ V s^{-1} at 25 °C. Coverage $\Gamma(C_0^*)$: (a) 1.3×10^{-7}, (b) 6.5×10^{-7}, and (c) 26×10^{-7} mol cm^{-2} of the ferrocene site

voltammograms of the low-, moderate-, and high-coverage $PFDMS_{20}$-*b*-$PDMS_{200}$ film on a glassy carbon electrode in aqueous $LiClO_4$ are shown in Figure 5.

Striking changes occurred, at low and high coverage; two pairs of peaks were incorporated into a pair of inconspicuous broad peaks which shows that the redox reaction became difficult. Figure 6 also indicates ΔE_P is bigger at low and high coverage than it is at moderate coverage. At low coverage, the peak currents, i_{pc}, increased with increasing film thickness and then decreased at moderate coverage, at the same scan rate. But at high coverages, no variation of the peak currents with films thickness was observed. The relationship between i_{pc} and PFDMS-*b*-PDMS film coverage $\Gamma(C_0^*)$ is shown in Figure 6. At low coverage, the electrode surface was incompletely covered; therefore, electrolyte penetration and mass diffusion proceeded fast and unhindered as the amount of electroactive species on the electrode surface increased with increasing thickness. Therefore, as expected, i_{pc} increased with increasing film thickness until decreasing at moderate coverage, and then constant peak currents were obtained. When the polymer films were thick enough, the electrode surface was covered completely, the diffusion layer was broad enough, and the concentration of the electrochemically active species in the diffusion layer was constant and PDMS also became constant. In addition, the peak currents depended on the diffusion rates of electroactive species and the reaction rate of the electrode processes; hence, i_{pc} was affected by temperature and scan rate and was independent of the thickness of the films, so we were able to record constant peak currents.

Effect of Temperature on CV Behavior of the PFDMS-*b*-PDMS Film. The shapes of the CV peaks became distorted with increasing temperature (Figure 7) which is not consistent

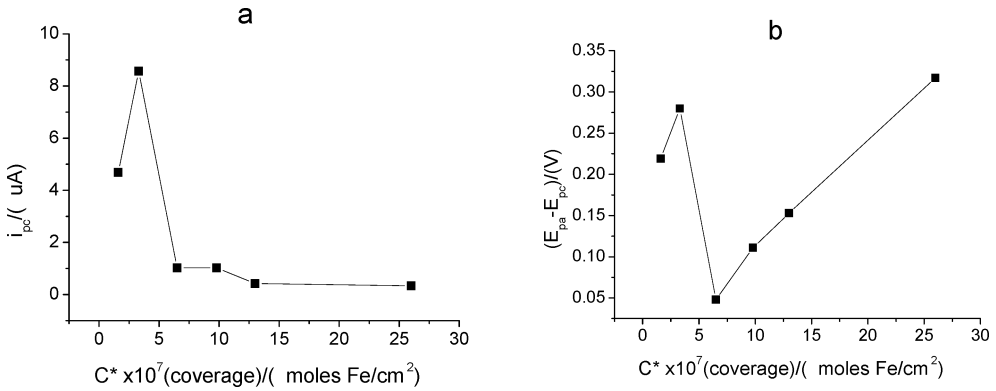

Figure 6. Influences of coverage on i_p and $E_{pa} - E_{pc}$ of the $PFDMS_{20}$-*b*-$PDMS_{200}$ film at a scan rate of 100 mV s^{-1} in aqueous 0.1 M $LiClO_4$ at 25 °C.

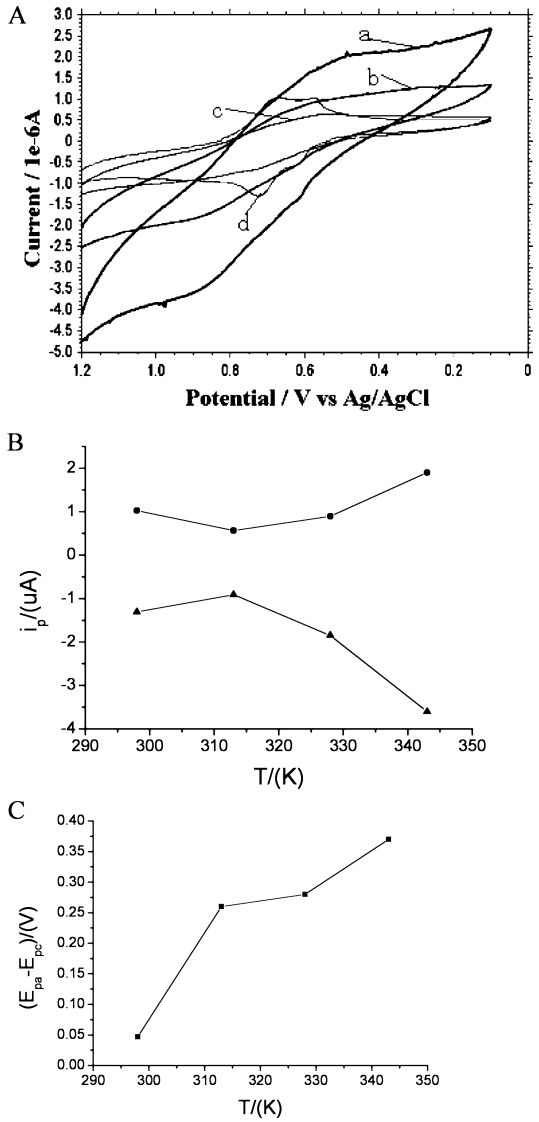

Figure 7. A. Cyclic voltammograms of the $FDMS_{20}$-*b*-$PDMS_{200}$ film in aqueous 0.1 M $LiClO_4$. Coverage Γ is 6.5×10^{-7} mol cm^{-2} of the ferrocene site, potential scan rate $v = 100$ mV s^{-1}: (a) 343, (b) 328, (c) 313, and (d) 298 K. B. Temperature influence on i_p. C. Temperature influence on E_p of the film.

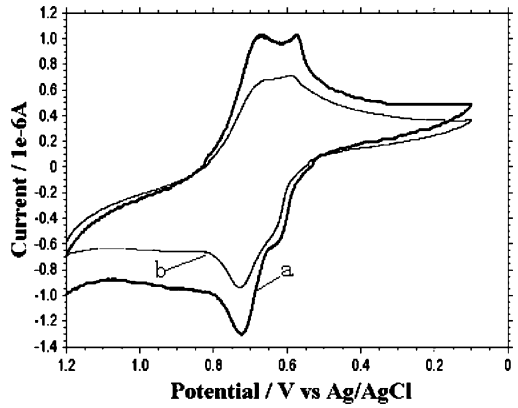

Figure 8. Cyclic voltammograms of the PFDMS-*b*-PDMS film on a glassy carbon electrode. Coverage Γ is ca. 6.5×10^{-7} mol cm^{-2} of the ferrocene site in aqueous 0.1 M $LiClO_4$ at a scan rate of 100 mV s^{-1} at 25 °C: (a) $PFDMS_{20}$-*b*-$PDMS_{200}$ film and (b) $PFDMS_8$-*b*-$PDMS_{270}$ film.

with the electrochemical behavior of a PFDMS film. The reduction peaks, E_{pc}, and oxidation peaks, E_{pa}, moved toward a lower potential value and a higher potential value, respectively. Thus, the peak-to-peak separation, ΔE_P, increased with increasing temperature; moreover, the reduction peak, E_{pc}, moved more than the oxidation peak, E_{pa}.

Both the oxidation and reduction peak current values decreased first and then increased with increasing temperature. The increase in current is likely to be controlled by the electrical conductivity of the solutions, the rate of diffusion, and the rate of electron transport. Therefore, the electrical conductivity of the solutions was measured in this temperature range. Results show that, from 25 to 70 °C, the electrical conductivity of the solutions increased from 4.8×10^{-3} to 7.5×10^{-3} S cm^{-1}, which is an increase of only 1.56 times. In contrast, the peak currents increased by much more to reach 2.77 times. This means that the segmental motion of the polymer chains, the rate of diffusion, and the rate of electron transport increased with raising temperature. Namely, the reversibility of the electrode reaction improved with increasing temperature.

Effect of Block Ratio on CV Behavior of the PFDMS-*b*-PDMS Film. CVs of PFDMS-*b*-PDMS films possessing different block ratios were investigated in aqueous $LiClO_4$. Typical cyclic voltammograms of the films on glassy carbon electrodes recorded in 0.1 M aqueous $LiClO_4$ at 25 °C are shown in Figure 8.

Previous CV studies of polyferrocenylsilanes have shown the presence of two reversible oxidation waves, indicating the presence of cooperative interaction between the iron centers.[17,18] The typical two-wave reversible pattern was also observed for $PFDMS_{20}$-*b*-$PDMS_{200}$ film even though the oxidation wave was not a 1:1 ratio. The $E_{1/2}$ values for the first and second oxidation

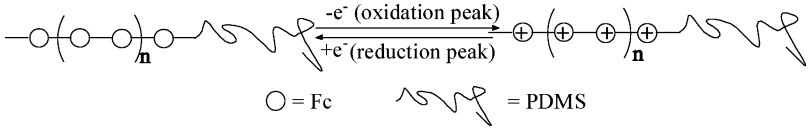

Figure 9. Schematic representation of the redox behavior of PFDMS-*b*-PDMS.

TABLE 4: Relationships of Peak Currents, Peak Potentials, and Potential Scan Rates of PFDMS-*b*-PDMS Films[a]

film	thickness (mol of Fe cm^{-2})	rate range (v) (V s^{-1})	linear equation (μA)	correlation coefficient (r)
$PFDMS_{20}$-*b*-$PDMS_{200}$	6.5×10^{-7}	0.01−1.0	$i_{pa} = -0.729 - 20.95v^{1/2}$	0.9968
			$i_{pc} = -0.257 + 19.641v^{1/2}$	0.9983
$PFDMS_8$-*b*-$PDMS_{270}$	6.5×10^{-7}	0.01−0.6	$i_{pa} = 1.476 - 16.601v^{1/2}$	0.9954
			$i_{pc} = 2.723 + 8.733v^{1/2}$	0.9958

[a] Temperature is 25°C.

waves were $E_{1/2}(1) = 0.626$ V and $E_{1/2}(2) = 0.724$ V, with a peak separation ΔE of 0.098. This peak separation is indicative of the degree of interaction between the metal centers.[25] Although the electrochemical behavior of the PFDMS homopolymer and PFDMS-*b*-PDMS in a solution of CH_2Cl_2 and MeCN have been found to be similar, the ΔE values are not consistent with the values previously reported for PFDMS-*b*-PDMS (0.27−0.29)[16] which shows that the PFDMS-*b*-PDMS film and PFDMS-*b*-PDMS solution have some differences in the oxidation process. The second oxidation process of the film was easy. The two-wave pattern in the CV can be attributed to the fact that oxidation of the alternating iron sites occurs first ($E_{1/2}(1)$), and the subsequent oxidation occurs adjacent to the two previously oxidized sites at a higher potential ($E_{1/2}(2)$). However, the peak separation of the ΔE is far smaller than that of PFDMS-*b*-PDMS in solution. Thus, it may be possible that $PFDMS_{20}$-*b*-$PDMS_{200}$ on a glassy carbon electrode exhibits different electrochemical behavior; it possesses only a single reduction and oxidation peak. For the sample of $PFDMS_{20}$-*b*-$PDMS_{200}$ especially, the distinguishable deposition and desorption on the film−electrode surfaces could be observed in the process of CV. The cause may not be that the oxidation occurs in one step but that the two steps cannot be distinguished on the time scale of the CV scan slow electron transfer. The possible oxidation process of $PFDMS_{20}$-*b*-$PDMS_{200}$ films is shown in Figure 9. Moreover, the electrochemical behavior of the PFDMS-*b*-PDMS film was strongly affected by the PFDMS content in PFDMS-*b*-PDMS. When compared with $PFDMS_{20}$-*b*-$PDMS_{200}$ with a high PFDMS content, $PFDMS_8$-*b*-$PDMS_{270}$ with a close M_n and a lower PFDMS content has no obvious deposition and desorption (Figure 8).

Kinetic Parameters of the PFDMS-*b*-PDMS Film Electrode Process. In aqueous $LiClO_4$, it was found that the CV peak current values, i_p, of the PFDMS-*b*-PDMS films were proportional to the square root of the scan rate ($v^{1/2}$) over a wide rate range. The linear range of the linear equation for the $PFDMS_{20}$-*b*-$PDMS_{200}$ film was much wider than that of the linear equation for the $PFDMS_8$-*b*-$PDMS_{270}$ film (Table 4). These relationships indicate that the charge transport through the films obeys Fick's law. The electrode processes of the films are diffusion controlled.[26]

Compared to the oxidation peaks, the reduction peaks were widening and shifting negatively much more, so that the apparent formal potential, E_0', where $E_0' = (E_{pc} + E_{pa})/2$, shifted to slightly more negative potentials with increasing scan rate. The relationship between the peak potential ($E_p - E_0'$) and the logarithm of potential scan rate ln v of the $PFDMS_{20}$-*b*-$PDMS_{200}$ film is shown in Figure 10. The $PFDMS_8$-*b*-$PDMS_{270}$ film

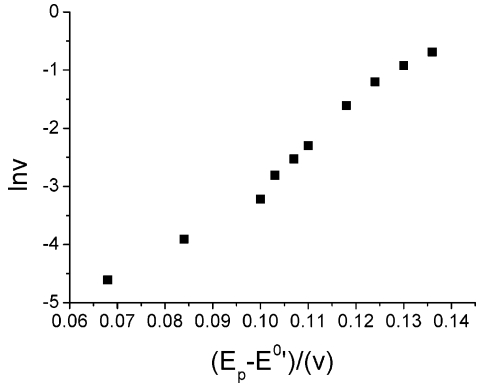

Figure 10. Peak potential of the PFDMS-*b*-PDMS film vs the rate of potential scan. Coverage $\Gamma = 6.5 \times 10^{-7}$ mol of Fe cm^{-2} in aqueous 0.1 M $LiClO_4$ at 25 °C.

exhibited similar trends. The peak potentials of the film shifted with increasing potential scan rate, but the relationship was nonlinear.

It is well-known that in a reversible electrode process, peak potential E_p is independent of scan rate and in a totally irreversible process there is a linear relationship between the peak potential and the logarithm of scan rate.[26] The above experimental results indicated that electrochemical processes of a PFDMS-*b*-PDMS film on a glassy carbon electrode were complex. These processes were neither simple reversible nor totally irreversible ones. It was shown that the rates of electron transport through the film and transfer between film and electrode were slow. Although the electrode processes were diffusion controlled, the rates of charge transport and the electrode reaction were rather slow. Because of the slow rates of charge transport when potential was scanned at low rate, the electrode reaction could reach completion and the CV exhibited nearly reversible features. But when the potential was scanned at higher rates, the electrode reaction could not reach completion in time; hence, the CV exhibited quasi-reversible or irreversible features, and this electrode process was controlled by both the electrode reaction and mass diffusion.

According to CV theory, [26] the relationships of the peak potential, peak current, and potential scan rate for an irreversible process are as follows:

$$i_p = 0.4958nF(\alpha n_\alpha)^{1/2}\left(\frac{F}{RT}\right)^{1/2} AD_0^{1/2}C_0^* v^{1/2} \qquad (1)$$

$$i_p = 0.227nFAC_0^* k^0 \exp\left[-\left(\frac{\alpha n_\alpha F}{RT}\right)(E_p - E_0')\right] \qquad (2)$$

where αn_α is the surface transfer coefficient, D^0 is the diffusion

TABLE 5: Kinetic Parameters of the Electrode Process for Three Films in 0.1 M Aqueous $LiClO_4$[a]

films	thickness (mol of Fe cm^{-2})	peak type	αn_α	D_{app} ($\times 10^{11}$ cm^2 s^{-1})	k^0 ($\times 10^7$ cm s^{-1})
PFDMS	6.5×10^{-7}	oxidation	0.766	37.9	147
		reduction	0.940	6.93	45.3
$PFDMS_{20}$-*b*-$PDMS_{200}$	6.5×10^{-7}	oxidation	0.310	0.472	7.25
		reduction	0.505	0.116	2.74
$PFDMS_8$-*b*-$PDMS_{270}$	6.5×10^{-7}	oxidation	0.284	0.422	5.34
		reduction	0.359	0.105	1.85

[a] Temperature is 25 °C.

coefficient of electroactive species (cm^2 s^{-1}), and k^0 is the standard rate constant (cm s^{-1}). Because the concentration of ferrocene sites in the film, C_0^*, cannot be measured accurately, we assumed an approximate film thickness $d = 10$ μm, and obtained $C_0^* = \Gamma/d$ mol cm^{-2}. We took the segment with a sufficiently high potential scan rate (0.1−0.5 V s^{-1}) where an approximately linear relationship between peak potential E_p and logarithm of scan rate ln v was obtained, namely, the irreversible region, to calculate the kinetic parameters. The calculated αn_α, D_{app}, and k^0 values are listed in Table 5.

The kinetic parameters obtained, the surface transfer coefficient, αn_α, the apparent diffusion coefficient, D_{app}, and the standard rate constant, k^0, of the films were extraordinarily small. They were smaller than the parameters obtained from the same polymers in solution. For example, D_{app} of the PFDMS in CH_2Cl_2 solution was ca. 10^{-6} cm^2 s^{-1}.[27] These results indicated that the diffusion rates of electroactive species and the rate of charge transport between the films and electrode were slow because the poorly solvent swollen high molecular weight polymer thick film hindered mass diffusion and interaction of active sites. This is the reason that electrode processes are irreversible at high scan rates.

In general, αn_α expresses the electrode surface electron exchange efficiency, i.e., the reversibility of the electrode process; αn_α affects the peak potentials and the symmetry of the curves.[26] With a decrease in αn_α, the cathodic peak shifts cathodically, the anodic peak shifts anodically, the peaks broaden, and the peak heights decrease. The rather small αn_α and k^0 revealed that the low rates of charge transport and low electron exchange efficiency at the electrode surface might be the major factors responsible for the low electrode reaction rate. By comparing the kinetic parameters of the two films, we noticed that most of the values for the PFDMS-*b*-PDMS films were smaller than those corresponding to the PFDMS films. In addition, most of the values for the $PFDMS_8$-*b*-$PDMS_{270}$ films were smaller than those corresponding to the $PFDMS_{20}$-*b*-$PDMS_{200}$ films. This is perfectly understandable because as in thin films the PFDMS in the block copolymer would exist in small phase-separated nanodomains within an insulating PDMS matrix. The PFDMS domains would likely be more isolated from the electrode, and slower electron transfer would be expected.[13,28] Thus, these small kinetic parameters indicate that the slower charge transport rates between the films and the electrodes and the lower electron exchange efficiency on the electrode surface were the major factors that caused the lower film electrode reaction rates and decreased reversibility of the PFDMS-*b*-PDMS film electrode processes.

Conclusions

The CVs of two kinds of polyferrocene block copolymer films, $PFDMS_{20}$-*b*-$PDMS_{200}$ and $PFDMS_8$-*b*-$PDMS_{270}$, on glassy carbon disk electrodes in aqueous $LiClO_4$ were recorded. Experimental results demonstrate that the counterion flow into and out of the solvent swollen polyferrocene block copolymer films is the rate-controlling process. Oxidation and reduction of fixed electroactive sites generated charged sites in the polymer film for maintaining charge neutrality.

The kinetic parameters of the three films, αn_α, D_{app}, and k^0, are extremely small. This result indicates that the diffusion rates of active species and the rates of charge transport between films and electrodes are slow which can be attributed to the thick polymer films hindering the mass diffusion and interaction of the active sites. This makes the electrode process quasi-reversible or irreversible.

The PDMS chain in PFDMS-*b*-PDMS molecules blocks the mobile chains of the polymer and hinders electron transfer. This steric molecular configuration limits the rate of mass diffusion and the interaction of the electroactive sites in the PFDMS-*b*-PDMS films so that their kinetic parameters, especially αn_α, are smaller than those of the PFDMS films. Most numerical values of the above parameter for the $PFDMS_8$-*b*-$PDMS_{270}$ films were smaller than those corresponding to $PFDMS_{20}$-*b*-$PDMS_{200}$ films with increasing PDMS and decreasing PFDMS. Therefore, the shapes of the voltammetric peaks of $PFDMS_8$-*b*-$PDMS_{270}$ films are broader, both the cathodic and anodic peak potentials are more positive, and the peak-to-peak separation, ΔE_p, is larger than the corresponding parameter of the $PFDMS_{20}$-*b*-$PDMS_{200}$ films.

Acknowledgment. Financial support from the National Natural Science Foundation of China (No. 20174032) and the Science and Technology Program of Ningbo City are gratefully acknowledged.

References and Notes

(1) Manners I. *Science* **2001**, *294*, 1664.
(2) Maclachlan, M. J.; Ginzburg, M.; Coombs, N.; Coyle, T. W.; Raju, N. P.; Greedan, J. E.; Ozin, G. A.; Manners, I. *Science* **2000**, *287*, 1460.
(3) Manners, I. *Angew. Chem., Int. Ed. Engl.* **1996**, *35*, 1602.
(4) Wang, X. J.; Wang, L. *Prog. Chem. (Beijing)* **2002**, *14*, 486.
(5) Compton, D. L.; Rauchfuss, T. B. *Organometallics* **1994**, *13*, 4367.
(6) Wang, X. J.; Wang, L.; Wang, J. J. *J. Funct. Polym.* **2002**, *15*, 368
(7) Tang, H. D.; Qin, J. G. *Polym. Bull. (Beijing)* **2001**, *4*, 15.
(8) Wang, L.; Ye, C. Y.; Zhang, P. Y.; Pan, J.; Feng, L. X.; Wang, S. F.; Peng, T. Z. *J. Appl. Polym. Sci.* **2001**, *82*, 3258.
(9) Wang, L.; Wang, X. J.; Pan, J.; Feng, L. X. *J. Appl. Polym. Sci.* **2002**, *86*, 3508.
(10) Wang, L.; Ye, C. Y.; Zhang, P. Y.; Pan, J.; Feng, L. X.; Wang, S. F.; Peng, T. Z. *Eur. Polym. J.* **2002**, *38*, 531.
(11) Wang, L.; Pan, J.; Ji, B.; Feng, L. X. *Acta Polym. Sin.* **2000**, *6*, 788.
(12) Rulkens, R.; Ni, Y.; Manners, I. *J. Am. Chem. Soc.* **1994**, *116*, 12121.
(13) Massey, J. A.; Power, K. N.; Manners, I.; Winnik, M. A. *J. Am. Chem. Soc.* **1998**, *120*, 9533.
(14) Massey, J. A.; Temple, K.; Cao, L.; Rharbi, Y.; Raez, J.; Winnik, M. A.; Manners, I. *J. Am. Chem. Soc.* **2000**, *122*, 11577.
(15) Raez, J.; Manners, I.; Winnik, M. A. *J. Am. Chem. Soc.* **2002**, *124*, 10381.
(16) Wang, X. J.; Wang, L.; Wang, J. J. *J. Polym. Sci., Part B* **2004**, *42*, 2245.

(17) Wang, X. J.; Wang, L.; Wang, J. J.; Chen, T. *J. Phys. Chem. B* **2004**, *108*, 5627.

(18) Ni, Y.; Rulkens, R.; Manners, I. *J. Am. Chem. Soc.* **1996**, *118*, 4102.

(19) Power-Billard, K. N.; Spontak, R.; Manners, I. *Angew. Chem., Int. Ed.* **2004**, *43*, 1260.

(20) Power-Billard, K. N.; Wieland, P.; Schafer, M.; Nuyken, O.; Manners, I. *Macromolecules* **2004**, *37*, 2090.

(21) Wang, X. S.; Winnik, M. A.; Manners, I. *Angew. Chem., Int. Ed.* **2004**, *43*, 3703.

(22) Nguyen, M. T.; Diaz, A. F.; Dememnt'ev, V. V.; Pannell, K. H. *Chem. Mater.* **1993**, *5*, 1389.

(23) Rulkens, R.; Perry, R.; Lough, A. J.; Manners, I.; Lovelace, S. R.; Grant, C.; Geiger, W. E. *J. Am. Chem. Soc.* **1996**, *118*, 12683.

(24) Peckham, T. J.; Lough, A. J.; Manners, I. *Organometallics* **1999**, *18*, 1030.

(25) Foucher, D. A.; Honeyman, C. H.; Nelson, J. M.; Tang, B. Z.; Manners, I. *Angew. Chem., Int. Ed. Engl.* **1993**, *32*, 1709.

(26) Bard, A. J.; Faulkner, L. R. *Electrochemical Methods;* Wiley: New York, 1980; Chapter 6.

(27) Finklea, H. O.; Hanshaw, D. *J. Am. Chem. Soc.* **1992**, *114*, 3173.

(28) Raezn J.; Zhang Y.; Cao L.; Petrov S.; Erlacher K.; Wiesner U.; Manners I.; Winnik M. A. *J. Am. Chem. Soc.* **2003**, *125*, 6010.